Virology 476 (2015) 226–232

Contents lists available at ScienceDirect

Virology

journal homepage: www.elsevier.com/locate/yviro

Specific nucleotides at the 3′-terminal promoter of viral hemorrhagic septicemia virus are important for virulence in vitro and in vivo

Sung-Hyun Kim [a], Tz-Chun Guo [a], Vikram N. Vakharia [b], Øystein Evensen [a,*]

[a] Norwegian University of Life Sciences, Faculty of Veterinary Medicine and Bioproduction, P.O. Box 8146 Dep, N-0033 Oslo, Norway
[b] Institute of Marine & Environmental Technology, University of Maryland Baltimore County, 701 East Pratt Street, Baltimore 21202, USA

ARTICLE INFO

Article history:
Received 9 August 2014
Returned to author for revisions
12 September 2014
Accepted 2 December 2014
Available online 30 December 2014

Keywords:
VHSV
Novirhabdovirus
3′-UTR
Promoter function
Virulence
In vitro
In vivo

ABSTRACT

Viral hemorrhagic septicemia virus (VHSV), a member of the *Novirhabdovirus* genus, contains an 11-nucleotide conserved sequence at the terminal 3′- and 5′-untranslated regions (UTRs) that are complementary. To study the importance of nucleotides in the 3′-UTR of VHSV for replication of novirhabdoviruses, we performed site-directed mutagenesis of selected residues at the 3′-terminus and generated mutant viruses using a reverse genetics approach. Assessment of growth kinetics and in vitro real-time cytopathogenicity studies showed that the order of two nucleotides (A4G5) of the 3′-terminus of VHSV directly affects growth kinetics in vitro. The mutant A4G-G5A virus has reduced total positive-strand RNA synthesis efficiency (51% of wild-type) at 48 h post-transfection and 70 h delay in causing complete cytopathic effect in susceptible fish cells, as compared to the WT-VHSV. Furthermore, when the A4G-G5A virus was used to challenge zebrafish, it exhibited reduced pathogenicity (54% lower end-point mortality) compared to the WT-VHSV. From these studies, we infer that specific residues in the 3′-UTR of VHSV have a promoter function and are essential to modulate the virulence in cells and pathogenicity in fish.

Introduction

Viral hemorrhagic septicemia virus (VHSV) of the genus *Novirhabdovirus* and the family *Rhabdoviridae* belongs to the order *Mononegavirales* (King et al., 2012). It has a linear non-segmented negative strand (NNS) RNA genome of 11 kb which contains the nucleocapsid protein (N), phosphoprotein (P), matrix protein (M), glycoprotein (G), RNA polymerase (L), and nonstructural NV gene (Schutze et al., 1999). The VHSV genome contains an 11 nucleotide-long, conserved sequences at the 3′- and 5′-termini that are unusual for high A/U content and complementary (Whelan et al., 2010). The terminal conserved and complementary sequences at the 3′- and 5′-termini are also found in other members of the order *Mononegavirales* (family *Rhabdoviridae*, *Filoviridae*, and *Paramyxoviridae*) (King et al., 2012). Based on vesicular stomatitis virus (VSV, the genus *Vesiculovirus* in the family *Rhabdoviridae*), it has been shown that the initiation of transcription and replication likely occurs at two different sites in the 3′-region of the virus (Whelan and Wertz, 2002; Chuang and Perrault, 1997;Qanungo et al., 2004). Furthermore, two polymerase complexes, one containing L and P and the other replicase complex containing N, P and L were proposed to control transcription and replication in VSV (Qanungo et al., 2004) but it is still unclear how the polymerase complexes are initiated at the 3′-terminus versus the N gene start (Galloway and Wertz, 2009). It is believed that the intracellular concentration of N that encapsidate the nascent leader RNA is a regulator for RNA-dependent-RNA polymerase (RdRp) activity switching from transcription to replication (Blumberg and Kolakofsky, 1981; Blumberg et al., 1983;Whelan et al., 2010).

In the family *Paramyxoviridae* and *Rhabdoviridae* (lyssavirus, rabies virus, and vesiculovirus), the terminal promoter regions have been shown to be multifunctional and not only are required for control of transcription and replication but also for encapsidation and assembly of newly synthesized RNAs (Whelan et al., 2010). However, no such information exists for the novirhabdoviruses and the underlying mechanisms governing the switch from transcription to replication mode have never been examined for the novirhabdoviruses. Our notion was that the conserved primary sequence which has A/U-rich content at the 3′- untranslated region (UTR) terminus may function as a potential promoter that could impact the transcription or/and replication of the virus (Grinnell and Wagner, 1984). We found that the 3′-UTR terminus nucleotides are 3′-C1AUA4G5UA7U8UUU11 and while C1AUA4 and U8UUU11 are complementary with the 5′-terminus, G5UA7 is not. The in silico secondary RNA structure is similar to the panhandle secondary RNA structure of influenza virus (*Orthomyxoviridae*) (Baudin et al., 1994) but there are no documentation in the literature that a panhandle structure is formed in novirhabdoviruses. We used this information as a guide and mutated the positions defined at the end and beginning of complimentarity (position 4 and 8 from the 3′ end) and beginning of non-complimentarity (positions 5 and 7), with the purpose to understand the importance of the 3′-terminal primary sequence for virus transcription and

* Corresponding author.

http://dx.doi.org/10.1016/j.virol.2014.12.003
0042-6822/

replication using site-directed mutagenesis and reverse genetics. The resulting mutant VHSVs were characterized by strand-specific quantitative RT-PCR (Matzinger et al., 2013;Purcell et al., 2006), growth kinetics, in vitro real-time cytopathogenicity, and challenge studies in zebrafish to assess the role of 3′- terminal specific sequence (A4G5) in replication and pathogenicity of the virus.

Results

Reduced RNA synthesis process rate of A4G-G5A corresponds with lower protein synthesis

To compare the viral protein expression level of VHSV mutants to that of rWT-VHSV (1st passage), the virus-specific N protein was detected in *Epithelioma papulosum cyprini* (EPC) cells by the indirect fluorescent antibody test (IFAT) (Fig. 1). The A4G-G5A variant exhibited reduced infectivity as evidenced by the reduced fluorescence (if any), whereas the other variants (A7C-U8A and U8C) yielded strong fluorescence which was comparable to rWT-VHSV (Fig. 1). The rescued viral titer of A4G-G5A variant (from supernatant) was 3 logs less than other variants and WT-VHSV control at 5 days post-transfection (not shown). To clarify the reason of the low infectivity of the A4G-G5A, we examined the efficiencies of RNA synthesis processes at 2 days post-transfection by using a strand-specific quantitative RT-PCR (ssqRT-PCR) to separately quantify the positive strand RNAs (mRNA and cRNA) and negative-strand RNA (viral RNA) at early time-points post-transfection. We anticipated that the reverse primer (−) would favor mRNA (+) and cRNA (+) levels while the forward primer (+) will favor negative-strand RNA expressions. We found that A4G-G5A variant had significant decrease of total positive-strand (51%) at 2 days post-transfection compared to a non-mutated control (rWT), while there was no difference indicating lower level of virus negative-strand (Fig. 2a). ssq RT-PCR will not differentiate between mRNA and cRNA and the CMV promoter will produce cRNA from the antigenome plasmid which may account for a portion of the measured RNA (+) by ssqRT-PCR. The relative contribution was shown to be minimal (< 1%) of the total cRNA using a control without pL helper plasmid (Fig. 2b). These findings are in favor of a reduction in cRNA synthesis in the A4G-G5A variant. By western blot viral proteins generated from mRNA (G and NV) are low at 2 days post-transfection (Fig. 3b) while present at 5 days post-transfection, expect for A4G-G5A where G protein is hardly discernible (Fig. 3b). Post-infection using rescued A4G-G5A showed delayed expression of N and P protein compared to WT-VHSV (Fig. 3a). Concurrently it took an additional 24 h for this variant to reach a viral titer comparable to WT-VHSV (Fig. 4).

3′-terminal mutations impact growth kinetics that corresponds with cytopathic effects of recombinant VHSV strains in vitro

The rescued recombinant VHSV strains (2nd passage) were then used to study infection kinetics in EPC (MOI = 0.1). A4G-G5A had a slower growth pattern (in conformity with what was shown for the viral protein expression; Fig. 3). We observed that A4G-G5A virus grew even slower with no increase in titer by 2 days post-infection, whereas the final titer was comparable to the WT virus (Fig. 4). These studies indicate that the A4G-G5A virus has delayed growth during early stages of infection.

To study the cell viability post-infection in real-time, we used the XCELLigence (Roche) system, which shows that U8C virus induced a drop in cell viability 4 h earlier than the WT-VHSV (Fig. 5a). For A7C-U8A virus, the loss of cell viability was delayed by 30 h and for A4G-G5A virus, the delay was 70 h, when compared to WT-VHSV (Fig. 5a).

Table 2
List of primers used for the point mutagenesis and quantitative RT-PCR.

Point mutation at 3′-terminal promoter[a]		Gene bank
A4G-G5A-Forward	gtcagatccgctagcgta CT ataaaagatgatgagttatgttac	
A4G-G5A-Reverse	gtaacataactcatcatcttttat AG tacgctagcggatctgac	
A7C-U8A-Forward	gtcagatccgctagcgtatca GT aaagatgatgagttatgttac	
A7C-U8A-Reverse	gtaacataactcatcatcttt AC tgatacgctagcggatctgac	
U8C-Forward	gtcagatccgctagcgtatcat G aaagatgatgagttatgttac	
U8C-Reverse	gtaacataactcatcatcttt C atgatacgctagcggatctgac	
3′-UTR-Forward	cattgacgcaaatgggcggta	
3′-RACE-Reverse	atccacgatcaccttcccatcatctg	
Strand-specific quantitative RT PCR		
VHSV-G-Forward	ggacacatgatcacagggtg	
VHSV-G-Reverse	gacagtttcttcgctccccc	
Carp-40s-Forward	ccgtgggtgacatcgttaca	AB012087
Carp-40s-Reverse	tcaggacattgaacctcactgtct	
Virus replication analysis (in zebrafish)		
VHSV-N-Forward	cgccatcatgatgagtcggatgctg	
VHSV-N-Reverse	cttctctgtcaccttgatcccctcc	
Zf-β-actin-Forward	atggatgaggaaatcgctg	AF025305
Zf-β-actin-Reverse	atgccaaccatcactccctg	

[a] Target nucleotides are in capital letter and red color.

Table 1
List of terminal RNA sequences of VHSVs and an in silico secondary RNA structure.

	RNA sequence[a]		Gene bank
Fil3 (genotype Ia)	3′-CAUAGUAUUUUCUA	UAAUAAAAGAUAUG_-5′	Y18263.1
23–27 (genotype Ia)	3′-CAUAGUAUUUUCUA	UAAUAAAAGAUAUG_-5′	FN665788.1
MI03GL (genotype IVb)	3′-CAUAGUAUUUUAUA	UAAUAAAAGAUAUGU-5′	GQ385941.1
JF00Ehi1 (genotype IVa)	3′-CAUAGUAUUUUCUA	UAGUAAAAGAUAUG_-5′	AB490792.1
KRRV9822 (genotype IVa)	3′-CAUAGUAUUUUAUA	UAAUAAAAGAUAUG_-5′	AB179621.1
JF-09 (genotype IVa)	3′-CAUAGUAUUUUCUA	UAGUAAAAGAUAUG_-5′	
Conserved sequence	3′-CAUAGUAUUUU_UA	UA_UAAAAGAUAUG_-5′	
Complementary nucleotides		G^5UA^7	
	3′-CAUA[4]	U^8UUU	
	5′-GUAU	A AAA	
		A G	
in silico secondary RNA structure ($\Delta G = -8.43$)[b]	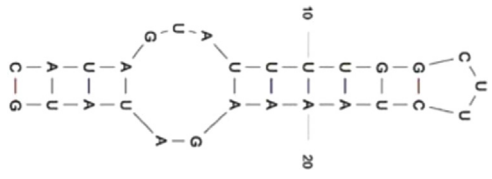		

[a] Different nucleotides among the VHSV RNA sequences are in italics and red color.
[b] The in silico secondary RNA structure was created by 'Mfold' web server.

Relative rate of virus replication of A4G-G5A virus was drastically lower (5%), compared to WT-VHSV at 72 h post-infection (Fig. 5b). Significant difference in cytopathic effect (CPE) was detected at 72 h post-infection between EPC cells infected with A4G-G5A and WT-VHSV (MOI=1) (Fig. 6).

All variants (A4G-G5A, A7C-U8A, and U8C) were sequenced by RACE with a GSP, 3′-RACE-Reverse (Table. 2), for the 3′-terminal nucleotides followed by a previously described method (Kim et al., 2014) with the purpose to ensure that the introduced mutation was still present following four passages in EPC cells. No mutation or reversion to wild-type was observed.

Pathogenicity studies in fish

To study if the observed attenuation would also impact in vivo virus virulence, we infected zebrafish with these viruses. Since it has been shown that VHSV is pathogenic to zebrafish after lowering of the water temperatures, we compared virulence of WT-VHSV and the A4G-G5A variant. Fish injected i.m. with 4×10^3 $TCID_{50}$ per fish (WT-VHSV) showed close to 90% cumulative percent mortality (CPM) over a period of 15 days post-challenge in zebrafish (Fig. 7a). When fish were injected i.p., the CPM was 83.3%. When the injection dose was lowered to 4×10^2 $TCID_{50}$ per fish (WT-VHSV) by i.m. and i.p., both gave 72.2% CPM. Injection of 4×10^3 and 4×10^2 $TCID_{50}$ per fish of A4G-G5A, i.p. resulted in 37.0% and 18.5% CPM, respectively (Fig. 7a), lowered by more than 50% compared to the WT-VHSV. There was also a delay in onset of mortality by almost 7 days (Fig. 7a). When the dose was lowered to 4×10 $TCID_{50}$ per fish for the A4G-G5A strain, no mortality was seen over a period 15 days post-challenge. All dead fish had signs of typical VHSV infection, hemorrhagic septicemia, ascites, and exophthalmia. VHSV was detected and confirmed from randomly sampled dead fish by cell culture and RT-PCR. A4G-G5A was detected at early time post-infection by RT-PCR only in fish infected with high-doses (Fig. 7b).

Discussion

Here we show that the primary sequence at 3′-terminus of VHSV is important for production of virus progeny in cell culture and pathogenicity in zebrafish. It has been shown that VSV, a prototype of the family *Rhabdoviridae*, has conserved complementary sequence of 3′- and 5′-termini which have been studied to understand RNA synthesis processes (Whelan et al., 2010). A single entry model predicts that a single polymerase entry site is located at the extreme 3′-terminus to make mRNA or copy viral RNA genome (Emerson, 1982). Later studies have shown that there are different sites initiating transcription and replication in the 3′-UTR of VSV (Whelan and Wertz, 2002;Chuang and Perrault, 1997; Qanungo et al., 2004). In NNS RNA viruses, the gene order is conserved with N, P, and M genes near the 3′-terminus and L gene at the 5′-terminus. The 3′-terminus promoter sequence seems a major determinant for control of gene expression in the viral life cycle (Whelan et al., 2010). The 3′- and 5′-termini of NNS RNA viruses contain specific sequences required for encapsidation of the RNA strand, binding of the RdRp, leader synthesis, transcription, replication, and assembly/budding of viral particles (Whelan et al., 2010). For VSV, positions 47–50 of the 3′-UTR leader-N gene junction were found essential for transcription and positions 15–50 at the terminus were dispensable for replication (Whelan and Wertz, 1999). Another study indicated that the signals for both transcription and replication for VSV were contained and overlapped within positions 1–24 at the 3′-terminus and positions 25–47 were needed for optimal transcription (Li and Pattnaik, 1999). There are no previous studies addressing the involvement of the terminal UTRs of novirhabdoviruses. Here we aimed at elucidating the importance of some positions of the primary sequence of the 3′-terminus of VHSV for virus propogation in vitro and in vivo pathogenicity using an in silico approach (Table 1). To differentiate between the positive-strand RNA (mRNA or cRNA) and negative-strand RNA (vRNA) formation, we used a previously published the ssq RT-PCR method (Matzinger et al., 2013;Purcell et al., 2006). The A4G-G5A in 3′-terminus had a significant negative effect (51% of rWT) on total positive-strand RNA synthesis (mRNA or cRNA) at 2 days post-transfection (Fig. 2). However, we cannot clearly differentiate between mRNA (transcription) and cRNA (replication) synthesis by ssqRT-PCR although the western blot studies are indicative of lower protein synthesis in the attenuated variant (A4G-G5A). We would need to follow up using an RNA assay (like Northern blotting) to differentiate between transcription and replication. Furthermore, A4G-G5A showed delayed expression of N and P protein post-infection compared to WT-VHSV (Fig. 3) and it took 5 days for this variant to reach a viral titer ($10^{7.55}$ $TCID_{50}$/ml) comparable to WT-VHSV ($10^{7.88}$ $TCID_{50}$/ml) which plateaued at 4 days post-infection, likely due to running out of available cells to infect (Fig. 4). Concurrent with this observation, the A4G-G5A variant also induced full CPE 70 h later than WT-VHSV (Fig. 5a).

As mentioned earlier, previous studies are indicative of transcription and replication being initiated at different sites for VSV, transcription initiated at the start of the N-gene (Whelan and Wertz, 2002; Chuang and Perrault, 1997;Qanungo et al., 2004). Moreover, there is an alternative possibility that RdRp always enters at the 3′-terminus (scanning) but the transcription is initiated at the start of the N-gene regardless of the 3′-terminus specific sequence (Whelan et al., 2010). The template-dependence of NNS RNA viruses for the RNA synthesis initiation is found to vary. Initiation of VSV is dependent on the first two nucleotides at 3′-terminus while for respiratory syncytial virus (RSV, *Paramyxoviridae*) initiation is independent of the first two nucleotides on the promoter terminus (Morin et al., 2012;Noton and Fearns, 2011). The transcription of RSV polymerase could be initiated at the 3rd nucleotide of the 3′-terminal promoter unlike that of VSV (Tremaglio et al., 2013) and the RSV polymerase–promoter interactions display sophisticated mechanisms for the viral promoter activity (Noton et al., 2012;Tremaglio et al., 2013).

Our findings would be suggestive of the initiation of replication is affected by the primary sequence near the 3′-terminus for VHSV and positions 4 and 5 play a key role like that of VSV (Whelan and Wertz, 2002;Chuang and Perrault, 1997;Qanungo et al., 2004;Whelan and Wertz, 2002) and these mutation were found genetically stable. While it is still not fully understood how the 3′-terminal sequences regulate transcription or/and replication efficiency for NNS RNA viruses in general, we are just beginning to understand how the 3′-terminus regulates these mechanisms for VHSV. This study showed that the primary sequence is an important promoter but it is not sufficient to document the importance of any secondary RNA structure (like double strand RNA promoter). The RNA synthesis profile should be examined to distinguish between effects of primary sequence versus secondary structure.

The introduced mutations at the 3′-terminus of VHSV affect formation of virus progeny in vitro and this is also corroborated by in vivo studies. We used the zebrafish model to study the impact of mutations on pathogenicity. It has been shown previously that VHSV is pathogenic to adult zebrafish (Encinas et al., 2010; Novoa et al., 2006) when the water temperature is lowered to 18 °C and below. The attenuation for the A4G-G5A strain is consistent over two virus doses, 4×10^2–4×10^3 $TCID_{50}$ per fish, and for the two doses tested there is a marked drop in end-point mortality compared to wild type virus (Fig. 7). Injection of 4×10 $TCID_{50}$ per fish of the A4G-G5A variant does not result in mortality (Fig. 7).

In conclusion this is the first study to show the importance of some positions (A4G5) of the primary sequence at the 3′-terminus as a potential promoter that governs progeny formation in VHSV, the genus *Novirhabdovirus*, in vitro. Similarly it is important for in vivo virulence in zebrafish (Fig. 7).

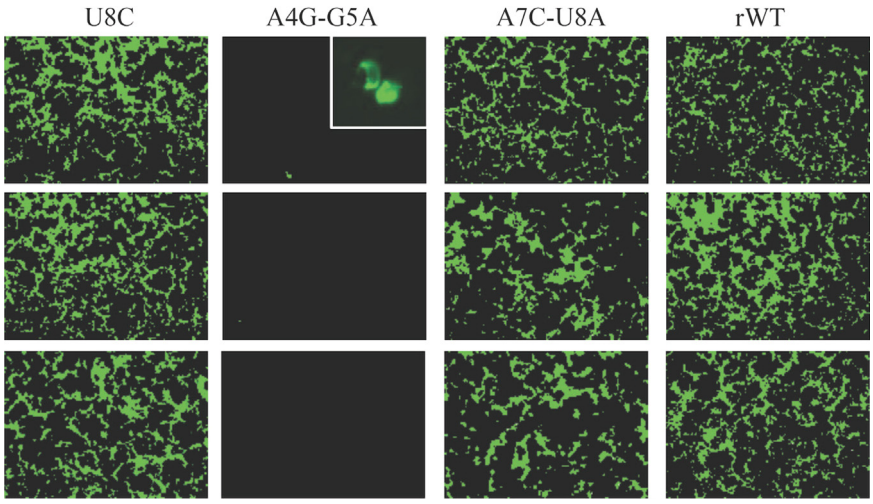

Fig. 1. Viral N protein expression of rescued recombinant VHSVs (1st passage; green fluorescence) in EPC cells (3 parallels) were shown by IFAT at 2 days post-infection. For the A4G-G5A variant, only a few cells showed positive fluorescence (shown in insert). A non-mutated recombinant VHSV (rWT) was used as a control.

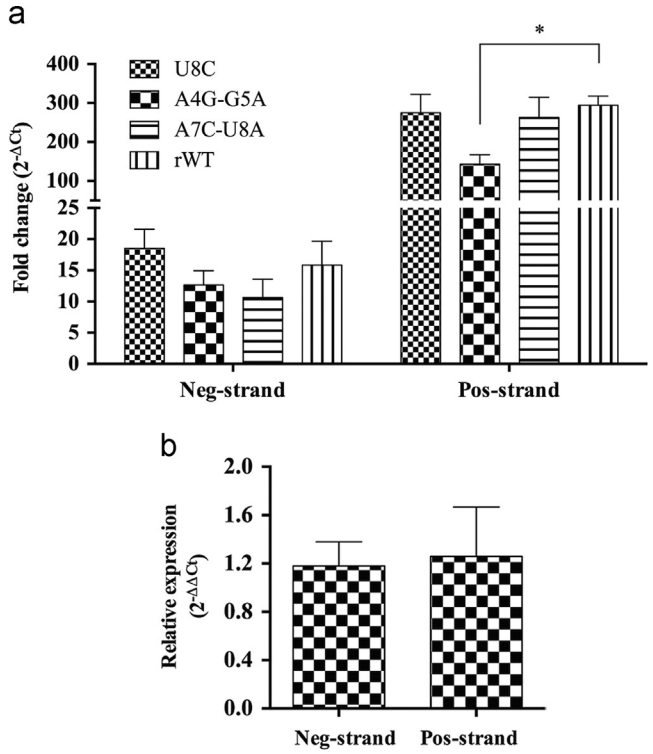

Fig. 2. Relative RNA quantification using strand-specific quantitative RT-PCR. a) Relative quantification of RNA using VHSV-G-Forward/Reverse of different mutants relative to a non-mutated control plasmid (rWT) at 2 days post-transfection. Negative- and positive-strand RNA quantification of mutated plasmids (A4G-G5A, A7C-U8A, and U8C). The results are expressed as mean ± SEM; $n=3$. An asterisk (*) denotes significant reduction ($P<0.05$) compared to a control reference (rWT). b) Relative quantification of A4G-G5A excluding pL (plasmid encoding the polymerase) showing background cRNA generation from plasmid (0.8% of pos-strand for A4G-G5A in a).

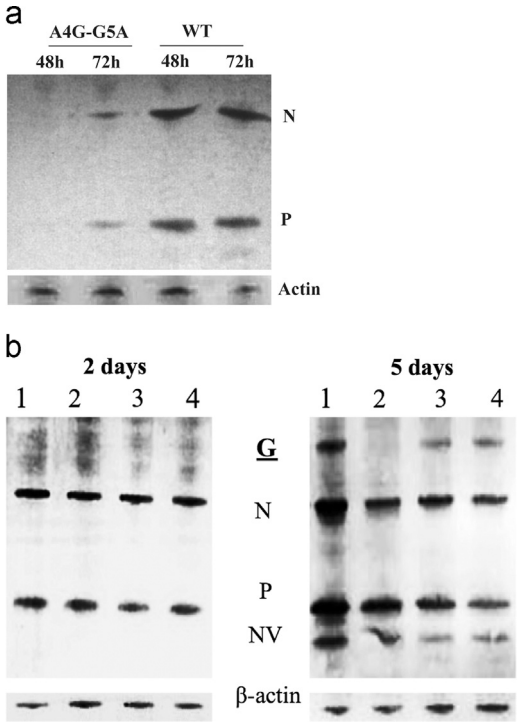

Fig. 3. Kinetics of viral protein expression of strain A4G-G5A. a) Viral specific proteins (Nucleocapsid protein, 42 kDa and Phosphoprotein, 26 kDa) of strain A4G-G5A and WT-VHSV in cell lysates were detected by western blotting post-infection of EPC cells (MOI=1), 48 and 72 h post-infection. b) Expression of VHSV proteins post-transfection by western blot using polyclonal antibody at 2 and 5 days post-transfection (lane 1: U8C, lane 2: A4G-G5A, lane 3: A7C-U8A, and lane 4: WT-VHSV).

Materials and methods

Virus and cells

VHSV (JF-09) was isolated from VHSV-infected olive flounder (*Plathychtis japonicus*) (juvenile) in a fish farm located in South Korea (June 2009) (Kim et al., 2014). The virus was propagated in *Epithelioma papulosum cyprini* (EPC) cells in L15 cell medium (Invitrogen) containing 10% FBS (Sigma-Aldrich) at 15 °C.

Site-directed mutagenesis

VHSV has conserved complementary RNA sequence in 3′-end (3′-CAUAGUAUUUU) and 5′-end (UAAAAGAUAUG-5′) (Table 1). By "introducing" a RNA hairpin loop, 3′-GGCUUC-5′, between conserved 3′- and 5′- terminal sequences, it was possible to predict an in silico secondary RNA structure by 'Mfold' web server (Table 1) (Zuker, 2003;Cheong et al., 1996, 1990;Varaniet al., 1991). Using the in silico secondary RNA structure as a guide, point-mutations were introduced mutations in positions A4G5 and A7U8 by site-directed mutagenesis (GENEART®, Invitrogen), referred to as A4G-G5A, A7C-U8A, and U8C. A previously constructed plasmid of

complete genome (rJF-09) (Kim et al., 2014) was used for this purpose. The point-mutated sequences were confirmed by sequencing (GATC Biotech) with GSPs (3′-UTR-Forward, Table 2).

Transfection and characterization of virus infection by IFAT

VHSV plasmids (250 ng), pN (60 ng), pP (50 ng), pL (50 ng), and pNV (30 ng) were mixed in 25 μl Opti-MEM® medium (Invitrogen) and 1.5 μl of FuGENE HD transfection reagent (Roche) was added. The mixtures were incubated for 10 min at room temperature and added to sub-confluent layers of EPC cells (1×10^5) in a 24-well plate. The cells were incubated at 28 °C for 5 h and then transferred to 15 °C and incubated further for desired time points or till cytopathic effects (CPE) was evident. The cell culture supernatants were collected at 4 days post-transfection, clarified by centrifugation, 10-fold diluted and inoculated onto EPC cells (2×10^5) in a 24-well plate. The cells were incubated at 15 °C for 48 h and fixed with of 4% paraformaldehyde for 20 min. The rescued viral N proteins were identified by using the standard indirect fluorescent antibody test (IFAT), using MAb IP5B11 as the primary antibody and Alexa 488 anti-mouse IgG (Molecular Probes, Invitrogen) as secondary antibody. The stained cells were washed and examined under an Olympus IX81 fluorescence microscope.

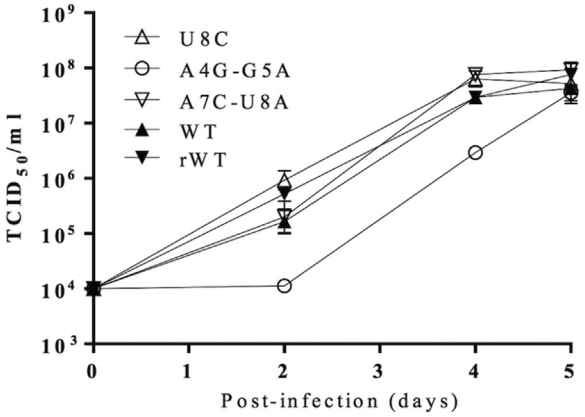

Fig. 4. In vitro viral growth pattern following infection of EPC cells (MOI=0.1). A non-mutated recombinant VHSV (rWT) and wild-type VHSV (WT) were used as a control. The titer values are presented as mean ± SEM from three parallels.

Strand-specific quantitative RT-PCR

Strand-specific quantitative RT-PCR (ssqRT-PCR) assay based on a published method (Matzinger et al., 2013;Troutt et al., 1992; Purcell et al., 2006) was modified for our study. VHSV plasmids (250 ng), pN (60 ng), pP (50 ng), pL (50 ng), and pNV (30 ng) were mixed in 25 μl Opti-MEM® medium (Invitrogen) and 1.5 μl of FuGENE HD transfection reagent (Roche) was added. The mixtures were incubated for 10 min at room temperature and added on sub-confluent layers of EPC cells (1×10^5) in a 24-well plate. The cells were incubated at 28 °C for 5 h and shifted to 15 °C. At 2 days post-transfection, the cells were harvested and total RNA were extracted from the cells by using a RNeasy® Plus Mini kit (Qiagen). To eliminate background plasmid DNA contamination prior to reverse transcription, the samples were DNase treated twice (TURBO DNA-free™ kit, Ambion). 11 μl of DNase treated total RNA was used as a template with a single GSP (0.5 μM), VHSV-G-Forward or VHSV-G-Reverse targeting G protein gene, in a final volume of 20 μl to create strand-specific cDNA templates (Transcriptor First Strand cDNA Synthesis kit, Roche). Quantitative RT-PCR was carried out by using LightCycler 480 SYBR green I master mix and LightCycler 480

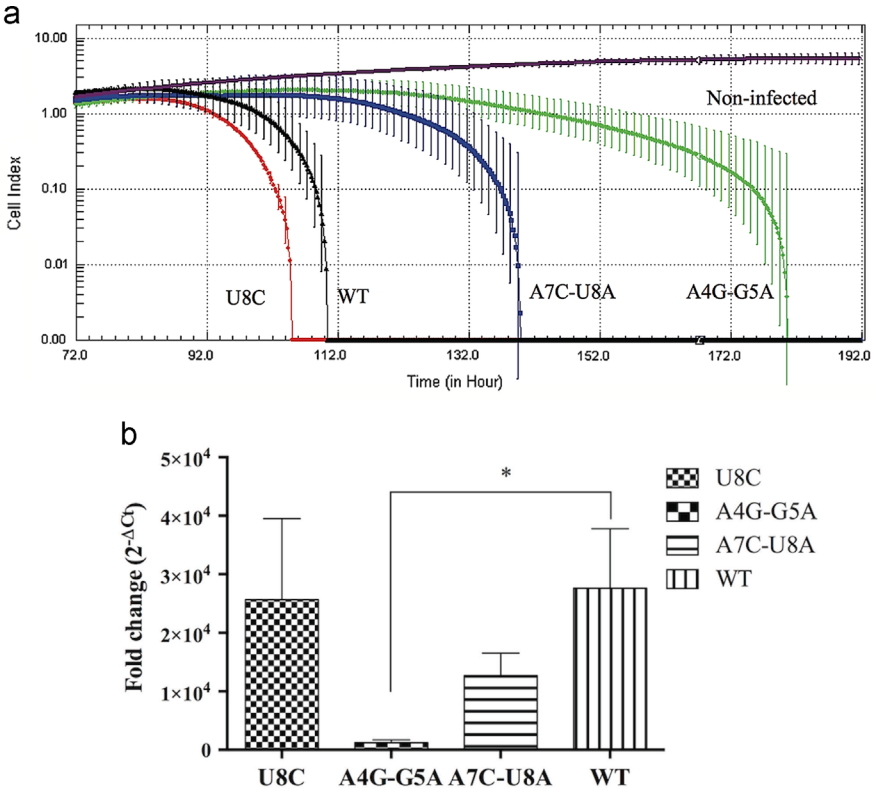

Fig. 5. Real-time cytopathic effects (CPE) of EPC cells after infection with recombinant VHSV strains (MOI=0.01). a) CPE was monitored in real-time by use of xCELLigence (see *Material and methods*). The results are expressed as mean ± SD ($n=3$). The first time point shown is 72 h post-infection since this was the earliest occurrence of reduced cell index (CI). b) Viral quantification in infected EPC cells (MOI=0.01) at 72 h post-infection by quantitative RT-PCR. The results are expressed as mean ± SEM ($n=3$). Wild-type VHSV (WT) was used as a reference. An asterisk (*) denotes significant reduction ($P<0.05$) compared to WT.

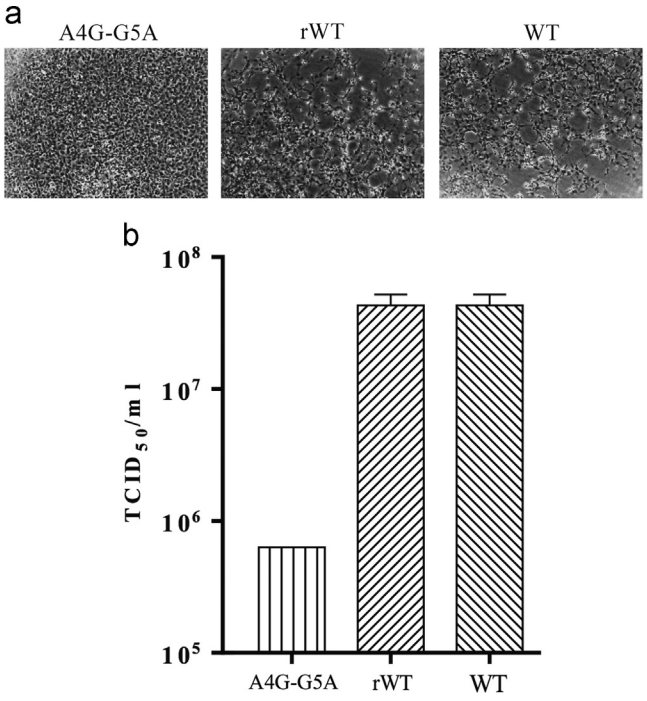

Fig. 6. a) Cytopathic effects (CPE) in EPC cells 72 h post-infection (MOI=1). b) The viral titer 72 h post-infection (mean ± SEM; n=3 parallels). A non-mutated recombinant VHSV (rWT) and wild-type VHSV (WT) were used as controls.

system (Roche). 2 µl of the strand-specific cDNA templates were used with a pair of GSPs (0.5 µM), VHSV-G-Forward and VHSV-G-Reverse, in a final volume of 20 µl. The mixtures were first incubated at 95 °C for 10 min, followed by 40 amplification cycles: 10 s at 95 °C, 20 s at 60 °C, and 8 s at 72 °C. Random hexamer primers (Transcriptor First Strand cDNA Synthesis kit, Roche) were used for cDNA templates for gene expression of carp 40 s, which is a reference gene to normalize the data (Joerink et al., 2006). The GSPs used for strand-specific quantitative RT-PCR are listed in Table 2. To compare the impact of pCMV driven cRNA synthesis from the plasmid relative to viral cRNA (polymerase), the A4G-G5A and rWT plasmids were transfected into the EPC cells without the pL helper plasmid followed by ssq RT-PCR.

Western blotting

EPC cells infected by A4G-G5A (2nd passage) and WT-VHSV (MOI=1) as described above and cells were lysed by using CelLytic M reagent (Sigma), at 48 and 72 h post-infection. Proteins were separated by SDS-PAGE and blotted onto a polyvinylidene difluoride (PVDF) membrane. The VHSV proteins were detected by western blotting using polyclonal antibody against VHSV (Ammayappan and Vakharia, 2011).

Growth kinetics

Growth kinetics was assessed by the $TCID_{50}$ method and the VHSV variants (2nd passage, MOI=0.1) were used to infect EPC cells (1×10^5) in 24-well plates in three parallels at 15 °C. After virus infection, the supernatants were collected at designated time points, clarified by centrifugation and titrated on EPC cells by the 50% tissue culture infective dose ($TCID_{50}$) method (Kärber, 1931).

For monitoring of cytopathic effects in real-time, VHSV variants (MOI=0.01) were used to infect EPC cells (1×10^4) in E-Plates (xCELLigence, Roche) in three parallels at 15 °C. The xCELLigence system showed a parameter termed 'Cell Index' which is derived as a relative change in measured electrical impedance and a correlate of cell status (integrity).

To measure viral replication in the cells by quantitative real-time RT-PCR, EPC cells (1×10^5) in a 24-well plate were infected by VHSVs (MOI=0.01) for the parallel sampling and collection was at 72 h post-infection, a starting point of CPE, at 15 °C. For the viral replication quantification, total RNAs were extracted from infected cells in a 24-well plate by using a RNeasy® Plus Mini kit (Qiagen). Quantitative real-time RT-PCR was carried out by using Quanti-Fast® SYBR® Green RT-PCR (Qiagen) and LightCycler 480 system (Roche). Total RNAs (10 ng) were used as templates with a pair of GSPs (1 µM), VHSV-G, in a final volume of 25 µl. The mixtures were subject to reverse transcription at 50 °C for 10 min, first incubated at 95 °C for 5 min and followed by 40 amplification cycles: 10 s at 95 °C, 30 s at 60 °C. Carp 40 s, which is a reference gene, was used to normalize the data (Joerink et al., 2006). The GSPs used for virus replication are listed in Table 2.

Pathogenicity studies in zebrafish

Wild-type zebrafish (*Danio rerio*) of 0.5–0.8 g (female:male=1:1) were obtained from the zebrafish experimental facility at the Norwegian University of Life Sciences. The fish were gradually transferred to lower water temperatures (1 °C per day) and kept to acclimate for 2 days at 16.5 ± 1 °C before virus infection. The water and feed were provided from the zebrafish facility. For each experiment, zebrafish were moved to closed aquaria (6 L) at 16.5 ± 1 °C and maintained at these conditions by water exchange (2 L) every day. The water quality was monitored by daily measurement of ammonia. The fish were

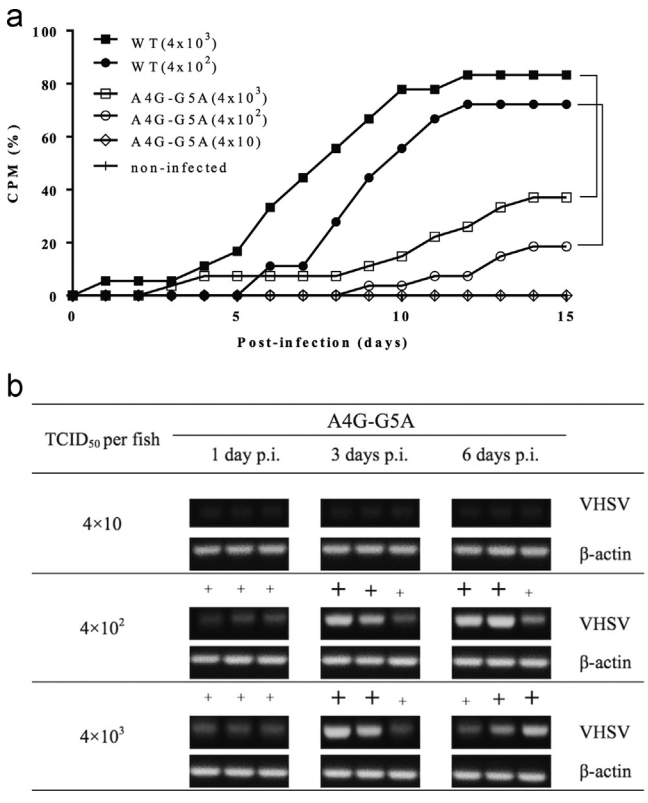

Fig. 7. a) In vivo viral pathogenicity in zebrafish. Cumulative percentage mortality (CPM) 15 days post-infection. Zebrafish were infected by intraperitoneal (i.p.) injection with WT-VHSV (WT), and A4G-G5A at three different doses; 4×10, 4×10^2 and 4×10^3 $TCID_{50}$ per fish. A non-infected control group was injected with 2 µl of L15 medium i.p.. Comparable infection groups are indicated by ']'. b) PCR amplicons (VHSV N gene) in A4G-G5A infected fish at 1, 3, and 6 days post-infection. Infection doses ($TCID_{50}$ per fish) are shown. Strength of bands is indicated semi-quantitatively.

anesthetized with benzocaine and injected intraperitoneally (i.p.) or intramuscularly (i.m.) at two infection doses for WT-VHSV (4×10^2 $TCID_{50}$ per fish or 4×10^3 $TCID_{50}$ per fish; 18 fish per group per dose) in three parallels using an injection volume of 2 μl and the fish injected i.p. at three infection doses for A4G-G5A variant (4×10 $TCID_{50}$, 4×10^2 $TCID_{50}$ or 4×10^3 $TCID_{50}$; all doses per fish; 36 fish per group per dose) in three parallels using an injection volume of 2 μl. Control groups were anesthetized and injected with 2 μl of L15 medium. Randomly selected healthy fish without gross pathology were decapitated and the whole organs were collected for virus detection by RT-PCR at early time post-infection. The selected fish (9 fish per group) were excluded from estimation of cumulative mortality. The GSPs used for virus replication are listed in Table 2.

Data analysis

The comparative delta delta Ct ($2^{-\Delta\Delta Ct}$) method was used to calculate relative difference of the RNA synthesis in this study (Livak and Schmittgen, 2001). Specificity of the PCR products was ensured by checking the melting temperature and profile of each melting curve. A *t* test was used to calculate differences with *P*-value < 0.05 considered as significantly different.

Acknowledgment

This study was partly supported by the Jeju Flounder Cluster, South Korea, and partly from the Research Council of Norway, Project no. 199813 “VHS virus – elucidation of pathogenic mechanisms” and Project no. 225293 “The importance of the UTR panhandle structure of VHS virus for replication and virulence”.

References

Ammayappan, A., Vakharia, V.N., 2011. Nonvirion protein of novirhabdovirus suppresses apoptosis at the early stage of virus infection. J. Virol. 85, 8393–8402.
Baudin, F., Bach, C., Cusack, S., Ruigrok, R.W.H., 1994. Structure of influenza-virus RNP.1. Influenza-virus nucleoprotein melts secondary structure in panhandle RNA and exposes the bases to the solvent. EMBO J. 13, 3158–3165.
Blumberg, B.M., Giorgi, C., Kolakofsky, D., 1983. N-protein of vesicular stomatitis-virus selectively encapsidates leader RNA invitro. Cell 32, 559–567.
Blumberg, B.M., Kolakofsky, D., 1981. Intracellular vesicular stomatitis-virus leader RNAs are found in nucleocapsid structures. J. Virol. 40, 568–576.
Cheong, C.J., Varani, G., Tinoco, I., 1990. Solution structure of an unusually stable RNA hairpin, 5′GGAC(UUCG)GUCC. Nature 346, 680–682.
Cheong, H.K., Cheong, C., Choi, B.S., 1996. Secondary structure of the panhandle RNA of influenza virus a studied by NMR spectroscopy. Nucleic Acids Res. 24, 4197–4201.
Chuang, J.L., Perrault, J., 1997. Initiation of vesicular stomatitis virus mutant polR1 transcription internally at the N gene in vitro. J. Virol. 71, 1466–1475.
Emerson, S.U., 1982. Reconstitution studies detect a single polymerase entry site on the vesicular stomatitis-virus genome. Cell 31, 635–642.
Encinas, P., Rodriguez-Milla, M.A., Novoa, B., Estepa, A., Figueras, A., Coll, J., 2010. Zebrafish fin immune responses during high mortality infections with viral haemorrhagic septicemia rhabdovirus. A proteomic and transcriptomic approach. BMC Genomics 11, 1–16.
Galloway, S.E., Wertz, G.W., 2009. A temperature sensitive VSV identifies L protein residues that affect transcription but not replication. Virology 388, 286–293.
Grinnell, B.W., Wagner, R.R., 1984. Nucleotide-sequence and secondary structure of VSV leader RNA and homologous DNA involved in inhibition of DNA-dependent transcription. Cell 36, 533–543.
Joerink, M., Ribeiro, C.M.S., Stet, R.J.M., Hermsen, T., Savelkoul, H.F.J., Wiegertjes, G.F., 2006. Head kidney-derived macrophages of common carp (*Cyprinus carpio* L.) show plasticity and functional polarization upon differential stimulation. J. Immunol. 177, 61–69.
Kärber, G., 1931. Beitrag zur kollektiven Behandlung pharmakologischer Reihenversuche. Naunyn-Schmiedeberg′s Arch. Pharmacol. 162, 480–483.
Kim, S.H., Thu, B.J., Skall, H.F., Vendramin, N., Evensen, O., 2014. A single amino acid mutation (I1012F) of the RNA polymerase of marine viral hemorrhagic septicemia virus changes the in vitro virulence to rainbow trout gill epithelial cells. J. Virol. 88, 7189–7198.
King, A.M.Q., Adams, M.J., Lefkowitz, E.J., Cartens, E.B., 2012. Virus Taxonomy: Classification And Nomenclature of Viruses: Ninth Report of the International Committee on Taxonomy of Viruses. Elsevier.
Li, T., Pattnaik, A.K., 1999. Overlapping signals for transcription and replication at the 3′ terminus of the vesicular stomatitis virus genome. J. Virol. 73, 444–452.
Livak, K.J., Schmittgen, T.D., 2001. Analysis of relative gene expression data using real-time quantitative PCR and the 2(T)(-Delta Delta C) method. Methods 25, 402–408.
Matzinger, S.R., Carroll, T.D., Dutra, J.C., Ma, Z.M., Miller, C.J., 2013. Myxovirus resistance gene A (MxA) expression suppresses influenza a virus replication in alpha interferon-treated primate cells. J. Virol. 87, 1150–1158.
Morin, B., Rahmeh, A.A., Whelan, S.P.J., 2012. Mechanism of RNA synthesis initiation by the vesicular stomatitis virus polymerase. EMBO J. 31, 1320–1329.
Noton, S.L., Deflube, L.R., Tremaglio, C.Z., Fearns, R., 2012. The respiratory syncytial virus polymerase has multiple RNA synthesis activities at the promoter. PlOS Pathog. 8, 1–13.
Noton, S.L., Fearns, R., 2011. The first two nucleotides of the respiratory syncytial virus antigenome RNA replication product can be selected independently of the promoter terminus. RNA 17, 1895–1906.
Novoa, B., Romero, A., Mulero, V., Rodriguez, I., Fernandez, I., Figueras, A., 2006. Zebrafish (Danio rerio) as a model for the study of vaccination against viral haemorrhagic septicemia virus (VHSV). Vaccine 24, 5806–5816.
Purcell, M.K., Hart, S.A., Kurath, G., Winton, J.R., 2006. Strand- specific, real-time RT-PCR assays for quantification of genomic and positive-sense RNAs of the fish rhabdovirus, Infectious hematopoietic necrosis virus. J. Virol. Methods 132, 18–24.
Qanungo, K.R., Shaji, D., Mathur, M., Banerjee, A.K., 2004. Two RNA polymerase complexes from vesicular stomatitis virus-infected cells that carry out transcription and replication of genome RNA. Proc. Natl Acad.Sci. USA 101, 5952–5957.
Schutze, H., Mundt, E., Mettenleiter, T.C., 1999. Complete genomic sequence of viral hemorrhagic septicemia virus, a fish rhabdovirus. Virus Genes 19, 59–65.
Tremaglio, C.Z., Noton, S.L., Deflube, L.R., Fearns, R., 2013. Respiratory Syncytial virus polymerase can initiate transcription from position 3 of the leader promoter. J. Virol. 87, 3196–3207.
Troutt, A.B., Mcheyzerwilliams, M.G., Pulendran, B., Nossal, G.J.V., 1992. Ligation-anchored PCR – a simple amplification technique with single-sided specificity. Proc. Natl. Acad. Sci. USA 89, 9823–9825.
Varani, G., Cheong, C.J., Tinoco, I., 1991. Structure of an unusually stable RNA hairpin. Biochemistry 30, 3280–3289.
Whelan, S.P.J., Barr, N.J., Wertz, G.W., 2010. Transcription and replication of nonsegmented negative-strand RNA viruses. In: Kawaoka, Y (Ed.), Biology of Negative Strand RNA Viruses: The Power of Reverse Genetics. Springer, pp. 61–119.
Whelan, S.P.J., Wertz, G.W., 1999. Regulation of RNA synthesis by the genomic termini of vesicular stomatitis virus: identification of distinct sequences essential for transcription but not replication. J. Virol. 73, 297–306.
Whelan, S.P.J., Wertz, G.W., 2002. Transcription and replication initiate at separate sites on the vesicular stomatitis virus genome. Proc. Natl. Acad. Sci. USA 99, 9178–9183.
Zuker, M., 2003. Mfold web server for nucleic acid folding and hybridization prediction. Nucleic Acids Res. 31, 3406–3415.